Chemical Science

ROYAL SOCIETY OF CHEMISTRY

EDGE ARTICLE

View Article Online
View Journal | View Issue

Cite this: *Chem. Sci.*, 2025, **16**, 22376

All publication charges for this article have been paid for by the Royal Society of Chemistry

Mechanoluminescence from amorphous solids of heteroleptic copper complexes and common luminophores induced by non-destructive mechanical stimuli and fabrication of flexible mechanoluminescent films

Ayumu Karimata, *[a] Daniil Ilatovskii, [a] Robert R. Fayzullin, [b] Shinya Komoto, [c] Andrew Bruhacs, [d] Eugene Khaskin [a] and Julia R. Khusnutdinova *[a]

A systematic study on mechanoluminescence in heteroleptic Cu^{I} complexes revealed that in the amorphous state, these complexes generate mechanoluminescence by friction as well as non-destructive stimuli such as contact–separation through an inert layer without direct physical damage to them, even under ambient air. No fracturing of the crystalline solids and no polymer matrix are required. Our findings overcome the limitations of the reported molecular crystalline mechanoluminescent materials generating luminescence by fracturing the crystalline solids, and enable a simple material design to develop non-crystalline flexible mechanoluminescent materials using photoluminescent molecules, which emit light under various non-destructive mechanical stimuli, including bending and twisting. The detailed study shows that the mechanism involves the generation of a strong electric field on the contact surface between two materials, caused by triboelectrification and contact electrification, which leads to the excitation of molecules.

Received 29th July 2025
Accepted 14th October 2025

DOI: 10.1039/d5sc05673j

rsc.li/chemical-science

Introduction

Mechanoluminescence (ML) or triboluminescence (TL) is a light emission phenomenon caused by mechanical stimuli. ML materials have been considered attractive components for mechanoresponsive materials used for visualization of damage and applied stress, friction, self-powered devices, or mechanical energy-converting technology because the luminescence is generated without light irradiation.[1–10] In the case of photoluminescent (PL) compounds, ML can be generated by fracturing the crystals (Fig. 1), which limits possible applications of this approach due to the decay of the ML intensity as the crystal breaks and its size decreases upon continuous stimulus, resulting in limited repeatability. There is also a dependence on the crystalline structure, which requires establishing the relationship between molecular structure and crystal design.

Several reports have shown that a mixture of a mechanoluminescent compound with a polymer matrix also exhibits ML.[11–16] Earlier, Demir *et al.* reported that microcrystals of known mechanoluminescent Cu^{I} or Eu^{III} complexes were required to observe ML by the impact of a steel ball on the polymer films containing them.[14,15] However, our group has demonstrated that cationic (pyridinophane)Cu^{I} N-heterocyclic carbene (NHC) complexes show bright ML in the crystalline state, as well as in amorphous, physically blended polymer films in the absence of a crystalline phase.[17] Later, triboelectrification of polymer matrices was found to enable versatile ML of common PL compounds in the blended amorphous polymer film by friction in the absence of a crystalline phase of the PL compounds.[18] However, the possibility of ML generation in pure

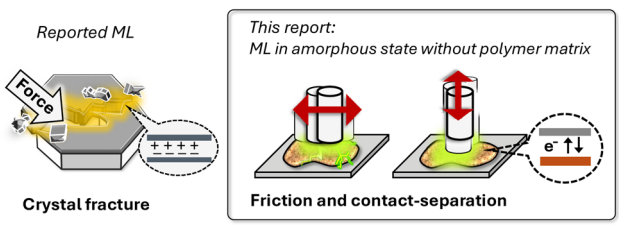

Fig. 1 Schematic illustration of the reported ML in PL compounds and this work.

[a]*Coordination Chemistry and Catalysis Unit, Okinawa Institute of Science and Technology, Graduate University, 1919-1 Tancha, Onna-son, Okinawa, 904-0495, Japan. E-mail: ayumu.karimata@oist.jp; juliak@oist.jp*

[b]*Arbuzov Institute of Organic and Physical Chemistry, FRC Kazan Scientific Center, Russian Academy of Sciences, 8 Arbuzov Street, Kazan 420088, Russian Federation*

[c]*Scientific Imaging Section, Okinawa Institute of Science and Technology, 1919-1 Tancha, Onna-son, Okinawa, 904-0495, Japan*

[d]*Engineering Section, Okinawa Institute of Science and Technology, 1919-1 Tancha, Onna-son, Okinawa, 904-0495, Japan*

amorphous PL solids without polymer matrices has not been investigated. Utilization of amorphous solids directly for ML can provide a simple and convenient preparation method that is universally applicable to a wide range of PL organometallic, inorganic, and organic compounds.

There are only a limited number of examples in PL compounds where transition metal complexes display ML, including Mn^{II},[16,19,20] Pt^{II},[21,22] Ir^{III},[18] Ru^{II},[23] and Cu^{I},[15,17,18,24–26] which is in stark contrast to the large number of reported organic compounds and rare-earth metal complexes.[2,4–6,9,27] Among them, metal complexes based on earth-abundant and inexpensive copper offer a practical alternative to precious metal- and rare-earth-based materials. In order to gain deeper insight into the mechanism of ML and develop bright and long-lasting ML materials, we performed a systematic investigation of a family of heteroleptic Cu^{I} complexes. These types of Cu^{I} complexes have previously been intensely studied in the context of their PL properties, including applications in photo-redox reactions, organic light-emitting diodes (OLEDs), and as sensors.[28–30] However, their ML properties have not been previously investigated in detail. Heteroleptic Cu^{I} complexes can be easily prepared, providing both cationic and neutral species, and show higher PLQYs compared to some homoleptic Cu^{I} complexes, which enables not only systematic study of ML but also developing practical and tunable ML materials. Herein, we demonstrate that ML can be easily generated by friction, contact-separation, and other types of stimuli (Fig. 1), in amorphous films made of pure heteroleptic Cu^{I} complexes even without a polymer matrix. Surprisingly, ML generated by friction is observed essentially across the entire studied family of Cu^{I} complexes; this is in contrast to their ML properties in the crystalline state, which were highly dependent on the crystal structure, clearly showing that ML in the amorphous state is governed by different factors. Our results suggest that triboelectrification (friction-induced electron transfer) and contact electrification are likely involved in the excitation of the Cu^{I} complexes in the amorphous films. The versatility of the ML generation by friction and contact–separation was also demonstrated using common luminophores that do not contain copper thus showing that these findings can generally be applied to a wider class of materials.

Results and discussion

Synthesis and preparation of amorphous solids of 1–8

In previously reported syntheses of heteroleptic Cu^{I} complexes, they were prepared from $[Cu^{I}(MeCN)_4]^{+}X^{-}$ ($X = BF_4$ or PF_6) and the corresponding ligands. Herein, we developed a more convenient synthetic procedure to obtain heteroleptic Cu^{I} complexes using readily available and inexpensive Cu^{I} chloride, which subsequently allowed facile counter anion variation (Scheme S1). $Cu^{I}Cl$ is combined with bis[2-(diphenylphosphino) phenyl]ether, then with the desired N-donor bidentate ligand followed by counter anion exchange or deprotonation with a base (if an NH group is present); the resulting complexes were isolated in 59–86% yields on a gram-scale. The PL properties and the charge of the complex can be easily tuned by the appropriate selection of the N-donor ligand. After analysis of the literature-reported complexes,[28–30] cationic complexes **1–5** [31–33] and neutral complexes **6–8** [33–35] were selected for this study (Fig. 2) as they reliably provide sufficiently large, millimeter-size crystals reproducibly and show good air- and thermal stability, which was confirmed by heating the acetone solution at 50 °C or acetonitrile solutions at 70 °C for 6 hours under air (Fig. S97–S100) and by thermogravimetric analysis (TGA) of the solids (Fig. S104–S106). Cu^{I} complexes **1–8** were characterized by NMR spectroscopy, single crystal X-ray diffraction, and powder X-ray diffraction (PXRD) analysis. All the obtained single crystal structures in this study are new,[36] except for previously reported **3**.[32] In the case of **8**, mechanoluminescent crystal modification **A** and non-mechanoluminescent crystal modification **B** were obtained. They could be selectively prepared by optimized crystallization under different conditions (see the SI). PXRD analysis of the bulk crystals of **1–8** confirmed the absence of polymorphs (Fig. S57 and S58).

Thin film-shaped amorphous solids of **1–8** were prepared by spin coating on a glass plate (thickness of the films: 0.6–2.4 μm, SI, Fig. S6). As references, (tris(8-hydroxyquinolinato) aluminium) (**Alq_3**) and 4,4′-bis(9*H*-carbazol-9-yl)biphenyl (**CBP**), which provide amorphous solids used for OLEDs,[37,38] were also investigated. Yokoyama *et al.* investigated the parameters, such as spin speed, solvents, and concentration of solution, to control the thickness of spin-coated amorphous films.[38] Based on this, the conditions to prepare amorphous films of **1–8** were optimized, and the details of film preparation of **1–8** are described in the SI. XRD analysis of the thin film-shaped solids on the glass plate showed the absence of crystalline phase peaks (Fig. 3). Mechano-induced crystallization of the amorphous solid was not observed by XRD analysis (Fig. S61).

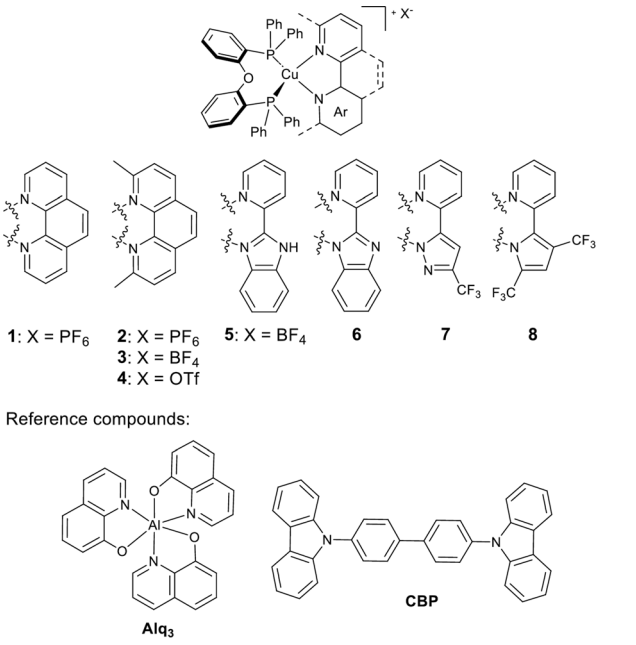

Fig. 2 Heteroleptic Cu^{I} complexes **1–8** and reference compounds Alq_3 and CBP used for this study.

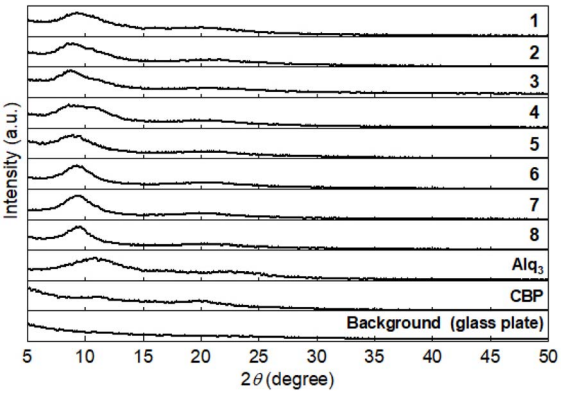

Fig. 3 XRD patterns of the amorphous thin films of **1–8**, **Alq_3**, and **CBP** on a glass plate.

Attempted preparation of amorphous solid glasses by melting–cooling resulted in their decomposition when heated near the melting points (200–300 °C) determined by differential scanning calorimetry (DSC) (Fig. S107 and S108), and was accompanied by color changes to brown or black.

Photoluminescence properties

Photoluminescence (PL) properties of **1–8** in the crystal and the amorphous state are summarized in Table 1. The photoluminescence quantum yield (PLQY) varies depending on the bidentate ligand (from 0.02 to 0.79). It has been reported that Cu^I complexes undergo large structural relaxation (distortion from tetrahedral to planar geometry) in the excited state, which results in the promotion of non-radiative decay, and can be suppressed by a rigid ligand structure, bulky substituents, or a rigid matrix, leading to an improvement of PLQY.[28–30] This general trend was also observed in complexes **1–8**. PL properties of **1–8** in solutions and polymethylmethacrylate (PMMA) are summarized in Tables S3, S4, Fig. S63 and S65–S67. For example, **1**, **5**, and **7** are non-PL in dichloromethane solution (PLQYs < 0.01), while they are moderately luminescent in the crystalline and amorphous states, as well as PMMA films (2 wt% of the Cu^I complex) (PLQY: 0.08–0.57). PLQY of **2–4**, and **8** are 0.27–0.41 in dichloromethane, and increase in both amorphous solids and crystals (PLQY: 0.48–0.75), accompanied by a blue-shift, which can be explained by the suppression of structural relaxation in the excited state. Among **1–8**, neutral **6** is an exception to this trend, showing lower PLQY in the crystalline and amorphous solids compared to solution and PMMA films (PLQY: 0.02 in crystal and amorphous, 0.52 in PMMA films, and 0.06 in CH_2Cl_2). This could be due to the overall neutral charge of the complex and the absence of a counter anion and bulky substituents on the ligand, which could make it more susceptible to intermolecular interactions in the solid state, lowering its PLQY.

Interestingly, the crystals of **6** and **8B** exhibit much longer PL lifetimes (**6:** 210 μs and **8B:** 270 μs under N_2) compared to **1–5**, **7**, and **8A** (10–52 μs under N_2) (Table S6 and Fig. S68–S70) and other reported heteroleptic Cu^I complexes.[28–30] Controlling the rates of intersystem crossing and radiative and non-radiative decay has been an important subject in studies of luminescent Cu^I complexes. Long PL lifetimes that are over a hundred microseconds at room temperature may be advantageous for visualization of damage and stress with ML. This is a rare property for Cu^I and has been confirmed only for five examples of heteroleptic Cu^I complexes,[39] and for recently reported two-coordinate Cu^I complexes bearing a carbene ligand.[40–42]

Table 1 Summary of PL and ML properties of **1–8** in crystalline and amorphous solids[a]

	In crystalline state[b]			In amorphous solid		
Cu	PLQY	PL λ_{max}	ML λ_{max}	PLQY[c]	PL λ_{max}[d]	ML λ_{max}[d]
1	0.26	585	593	0.09	597	606
2	0.79	559	546	0.48	550	557
3	0.77	533	546	0.48	550	556
4	0.69	545	567	0.49	553	560
5	0.17	561	n.d.	0.08	583	586
6	0.02	509	n.d.	0.02	575	590
7	0.57	528	n.d.	0.20	542	547
8A	0.75	517	520	0.49	536	537
8B	0.72	499	n.d.			

[a] PLQY: photoluminescence quantum yield. λ_{max}: maximum wavelength/nm. [b] Under air. [c] Under a nitrogen atmosphere. [d] Under an argon atmosphere. Excitation wavelength for PL spectra: 385 nm.

Mechanoluminescence in the crystalline state

ML was first investigated by grinding the same amount of millimeter-size crystals of **1–8B** (5×10^{-5} mol, 42–54 mg) using a glass rod in a glass tube under air. In order to systematically compare the irregularly blinking ML in the fracturing crystal (SI Movie 1), photographs of ML were taken by integrating the photons emitted from the crystals for 15 seconds in the dark under the same conditions. The results show no detectable luminescence from **5**, **6**, **7** and **8B** under air (Fig. 4). **8A** exhibits the strongest ML in this series. When the atmosphere is replaced with dry N_2 or argon, visible ML is observed for complexes **5** and **6**, but not for complexes **7** and **8B**. It has been proposed that piezoelectricity (polarity, or non-centrosymmetry) of the crystal may be important to generate an oppositely charged cracked surface that causes the excitation of molecules in the crystal (or surrounding gas). Investigation of the crystal space group of **1–8B** indicates that only the crystals of **2** ($P1$) and **8A** ($P1$) are polar (Table S2). The two polar crystals exhibit ML upon fracturing. However, the entire investigation of this Cu^I complex family reveals that even non-polar crystals such as **1** ($P2_12_12_1$), **3** and **4** ($P2_1/_c$) exhibit visible ML under air. In addition, **5** ($P2_1/_n$) and **6** ($P\bar{1}$) show visible ML under an inert gas atmosphere. However, among two crystalline modifications of the same complex, **8A** and **8B**, the non-polar **8B** shows no ML. Therefore, ML generation in crystals does not show a simple correlation with the polarity of the crystals based on the space groups. Several other reports, including ours, also confirmed that centrosymmetric (non-piezoelectric) crystals may show ML in the crystalline phase,[17,18,22,27] suggesting that no clear

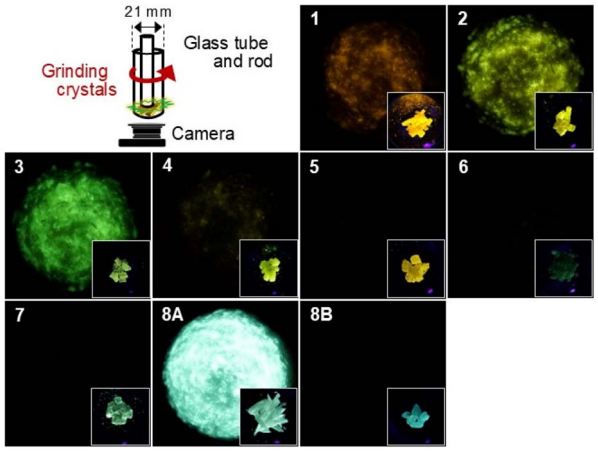

Fig. 4 Schematic illustration of the ML experiment and photographs of the crystals of **1**–**8B** being ground in the dark under air (the exposure time of the camera: 15 s), and the photographs of the pristine PL crystals before grinding under a UV lamp in the glass tube (inner diameter: 21 mm).

relationship between crystal structure and ML properties can be established. The most important observation arising from this, however, is that ML properties depend on the crystal structure, while they are not correlated with the presence or absence of ML in the amorphous state for the same compounds (see below). We have confirmed that ML is dependent on the particle size, with no ML observed when the particle size was less than 20 μm (Fig. S55).

ML spectra were measured by crushing the crystal with a glass tube that contains a fiber optic probe inside, which revealed shifts in the ML spectra compared to PL (Table 1). For example, ML of **1** shows a red-shift compared to PL, while that of **2** is blue-shifted. The shift of ML spectra can be due to the different environment resulting from mechanical grinding on the fractured surfaces, such as changes in crystal packing and intermolecular interactions, compared to the bulk pristine crystal.[22,43] To investigate this, we compared the ML spectra with PL spectra of well-ground micropowders with the particle sizes less than 20 μm (Fig. S55) that show no ML upon grinding with a glass rod and with the PL spectra of thin amorphous films made of the same Cu^I complexes (Table 1 and Fig. S81). This comparison indicates that ML spectra from the fractured crystals are not always in good agreement with the PL spectra of the ground powders and those of the amorphous solids. The photophysical properties of **1**–**8** are influenced by several factors (Table S4 and Fig. S65–S67), implying that the wavelength shift in ML of the Cu^I complexes cannot be simply explained by excitation of disordered molecules on the fractured crystal surface.

In order to gain further insight into the mechanism of ML, crystals of **1**–**6** and **8A** were ground under the flow of different gases, including N_2, Ar, He, CO_2, and a high dielectric strength gas, SF_6. Previous reports established that ML of non-PL crystals (such as sugars and inorganic salts) can be ascribed to the luminescence of discharging gases.[44–49] Based on this, one of the proposed mechanisms of ML observed in PL crystals suggests that excitation of PL molecules occurs by absorption of the light emitted from the generated gas plasma (mechano-photoluminescence).[3,4,49,50] ML spectra of **1**–**6** and **8A** under different gas flows show the presence of luminescence from gas discharge under Ar and He gas atmospheres (Fig. 5b and S74), which was compared against the luminescence spectra of gas discharge tubes (Fig. S71 and S75). Notably, ML intensity of **1**–**6** changes depending on the surrounding gas atmosphere (Fig. 5c, S74 and S76), showing more intense ML under Ar and He when compared to N_2, and a much weaker ML intensity under CO_2 and SF_6. This result confirms the correlation with the dielectric strength of the gas, and the luminescence efficiency of the gas plasma, as discussed in the previous reports.[49,50] However, in the case of **8A**, no apparent gas effect on ML intensity was observed (Fig. S76), implying that ML in crystals is not governed by a simple mechanism. In any case, these results indicate that ML properties of heteroleptic Cu^I complexes in the crystals are highly dependent on the crystal structure, without a clear correlation between ligand molecular structure, crystal structure, and ML properties.

The temperature dependence of the ML in the crystals was also investigated. The crystals of **1**, **3**, and **8A** were heated at 120 °C in an oven for 30 minutes, and then ground immediately before they cooled down under air. The heated crystal of **3** shows a significant decrease in ML intensity, while less dramatic changes were observed for the heated crystals of **1** and **8A** compared to the analogous experiments at RT (SI Movie 9).

We also examined the possibility of utilizing friction with macroscopic size crystals to generate ML. Complex **3** was selected for this experiment as it provided sufficiently hard crystals among the series **1**–**8B**. Although ML of **3** was confirmed by rubbing the two crystals against each other, or by rubbing a crystal against a plastic rod under an Ar atmosphere, this was accompanied by crystal fracture (Fig. S86 and SI Movie 3). Thus, in the case of friction using crystalline samples, it was not possible to separate ML generated by fracture and friction due

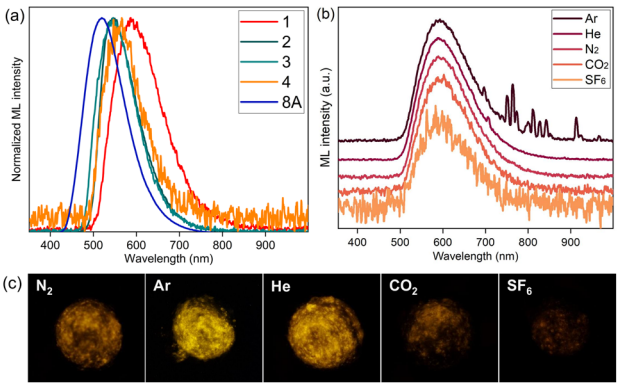

Fig. 5 ML spectra of crystals; (a) **1**–**4** and **8A** ground under air and (b) **1** ground under the flow of different gases. (c) Photographs of the crystals of **1** (47 mg, 5×10^{-5} mol) being ground with a glass rod in a Schlenk tube under different gas flows (the exposure time of the camera: 15 s).

to crystal fragility. Hence, the use of amorphous thin film solids described in the next section is advantageous for repeatedly generating ML by friction and avoiding the confounding factor of crystal fracture.

Mechanoluminescence in amorphous films

Despite several reports on ML from PL compounds blended in polymers,[11–16,18] there has been no example of PL compounds showing ML in an amorphous solid in the absence of polymer matrices. In this work, amorphous thin films made of Cu^{I} complexes **1–8** were successfully obtained by spin coating on a glass plate (Fig. 3 and S6). When the surfaces of amorphous **1–8** and the reference **Alq_3** were rubbed with a flexible silicone rod under an Ar atmosphere, visible ML was observed (Fig. 6). ML of **CBP** was generated by using a rod made of perfluoroalkoxy alkane (PFA) for efficient ML generation. The ML spectra, which were recorded by rubbing the surface using a PFA tube containing an optic fiber probe, consist of luminescence from the corresponding Cu^{I} complex along with intense luminescence from the surrounding gas discharge (Fig. 7a and S77). The presence of branching, lightning-like luminescence patterns in the ML from amorphous **1–8** films (Fig. 6, S78 and SI Movie 2) suggests that gas discharge induced by friction is involved in the ML. Gas plasma luminescence generated by tribo-charging during the friction of inorganic insulators or polymer materials has also been reported previously, in the absence of PL materials.[3,51–54]

The maximum wavelengths of ML peaks corresponding to the heteroleptic Cu^{I} complexes are red-shifted compared to the PL spectra (Table 1 and Fig. S85). Miyata *et al.* reported the generation of luminescence in fluorescent compounds blended in a host polymer, polyvinylcarbazole, by corona discharge under Ar gas,[55] in which a red-shift was observed and attributed to the effect of a high electric field (a few kV), based on a control experiment with and without applying voltage to the fluorescent compound on an anode. Similarly, the red-shift of **1–8** in amorphous films may be due to an electric field generated by triboelectrification, or because of the different environment on the surface as compared to the bulk solid. Amorphous films with varied thicknesses of 0.076, 0.528, and 1.46 μm were prepared by changing the concentration of the solution for spin-coating using **3**. When the films were rubbed with a silicone rod under an Ar gas atmosphere, no significant difference was observed for the ML intensity.

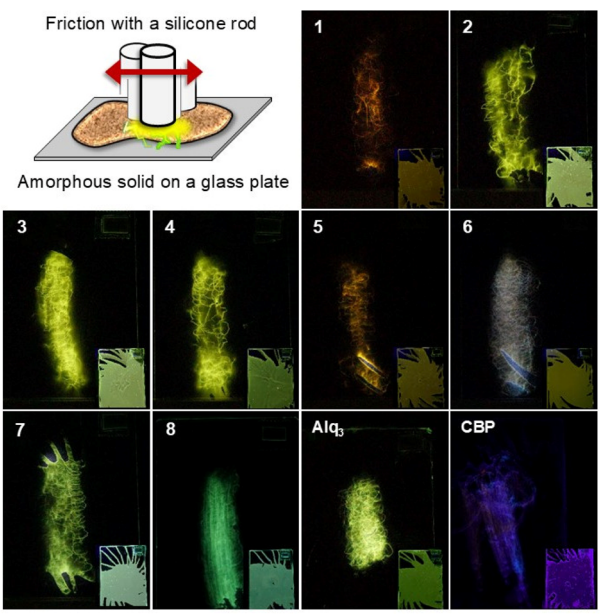

Fig. 6 Schematic illustration of ML experiments and the photographs of the amorphous solids **1–8**, **Alq_3**, and **CBP** being rubbed with a silicone rod (diameter: 10 mm) on a glass plate in the dark under an Ar atmosphere. The insets show the photographs of the solid under a UV lamp before the friction. The glass plates were held by hand against the glovebox window. The exposure time of the camera for ML is 10 s.

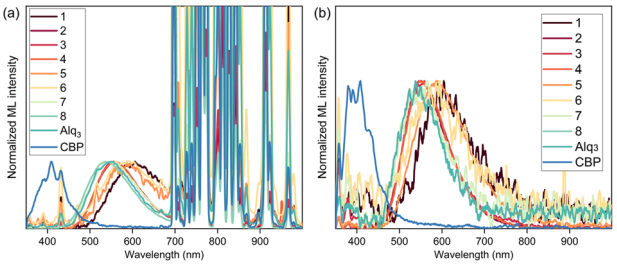

Fig. 7 ML spectra of the amorphous solids of **1–8**, **Alq_3**, and **CBP** on a glass plate: (a) direct friction under an Ar atmosphere with a PFA tube; (b) indirect friction with a glass tube *via* a PVC covering film placed on the surface of the films of amorphous solids under humid air (25 °C, relative humidity: 31–34%).

Importantly, ML of **1–8** is dependent on the materials used when generating ML by friction. Visible ML of **1–8** was observed when a rod made of PFA, polytetrafluoroethylene (PTFE), or polyvinylchloride (PVC), was used, which have been reported to be negatively charged by friction (Table S9),[54,56,57] while the use of glass, polymethylmethacrylate (PMMA), or polyethylene terephthalate (PET), which have been reported to become relatively positively charged based on the triboelectric series,[56,57] or polyethylene (PE) and polypropylene (PP), which bear no electron withdrawing group on the polymer chain, gave extremely weak or no detectable ML. Thus, we propose that triboelectrification between the PL amorphous solid film and the rod is involved in the generation of an electric field at the contact area, which leads to the excitation of PL compounds as well as gas discharge.

To generate ML in a more practical manner and to avoid direct physical damage to the amorphous solid film, ML generation by friction through an inert PVC layer was investigated. Previously, we demonstrated that ML of blended polymer films that contain common PL compounds is generated by friction even *via* an outer covering film that does not contain a PL compound.[18] When a PVC covering film (*ca.* 20–30 μm) is physically placed on top of the surface of the amorphous films of **1–8**, friction applied *via* the outer PVC film also generates ML from the inner PL amorphous solid, even under humid air (Fig. S80). In the ML spectra recorded under air in such

a double-film setup, the peaks of nitrogen gas discharge luminescence are observed in the UV region (Fig. 7b). Notably, when the outer film, which is made of PMMA, polystyrene (PS), polycaprolactone (PCL), or poly(bisphenol A carbonate) (PBAC), was used instead of PVC, ML was not observed. This result also indicates that the position of the polymer material in the triboelectric series is likely to be an important factor and suggests that triboelectrification may be involved in luminophore excitation. Interestingly, ML of cationic **1–5** is stronger than that of neutral complexes **6–8**, **Alq_3**, and **CBP** obtained by this method (see Fig. S80 and SI Movie 4 showing ML of amorphous **1–5** on a glass plate generated by rubbing the outer PVC covering film with a finger under air).

Generation of luminescence by contact–separation

For example, when a double-film setup consisting of a covering PVC film placed on top of the inner layer composed of amorphous solids of **1–5** was pressed lightly with a silicon rod (10 mm diameter), and the silicon rod was then removed, ML was generated under a humid air environment at the moment of separation (Fig. 8 and SI Movie 5). The ML was generated repeatedly and monitored using a CCD camera under air, showing a repeatable response over 90 cycles of contact–separation (*ca.* 1 Hz) without noticeable decay. According to the literature, gas discharge occurs between two insulators by contact electrification,[58–61] however, to the best of our knowledge, the generation of the excited state of PL compounds in amorphous solids upon separation has not been previously reported.

Although ML in polydimethylsiloxane (PDMS)-embedded semiconducting particles of ZnS:Cu[62] and ZnS:Mn[63] generated by compression–separation has been reported, this was attributed to the tilted band structure of ZnS:Cu, followed by the transition of the trapped electron caused by a triboelectrification-induced electric field[62] or to injection of electrons from the PDMS matrix to ZnS:Mn,[63] thus operating by different mechanisms. Recently, static electricity-induced luminescence of $SrAl_2O_4$:Eu_2 was reported, in which the luminescence was generated using an electrostatic generator without contact.[64] Another example is the mechano-induced bioluminescence, however; it was generated by compression.[65,66] The novelty of the current report is the observation of a robust and visible ML in response to contact-separation using amorphous, PL molecular solids.

Peeling off (separating) a PVC covering film placed on top of the surface of amorphous films of **1–8** also generates ML (Fig. 9 and SI Movie 6). While it is very well known that striping adhesive tapes also generate ML, usually attributed to luminescence of gas discharge or adhesive components,[46,67–69] no adhesive was required in our case; contrary to the adhesive peeling-off effect, the amorphous films composed of **1–8** exhibit no ML by peeling off adhesive tapes. The generation of ML can be caused by strong electric field induced by contact electrification,[58–61,67] between the amorphous solid and the PVC covering film. At the moment of separation, which generates oppositely charged surfaces due to contact electrification, the excitation of a Cu^I complex may occur by bombardment of electrons and ions or charge recombination caused by gas discharge. Interestingly, in the case of contact–separation, an apparent gas effect (N_2, Ar, CO_2, and SF_6) on ML intensity was not observed for **1–5**, probably due to a much stronger electric field exceeding the threshold of dielectric strength of the surrounding gas, or suggesting that gas discharge is not involved in the Cu^I luminophore excitation. Currently, the mechanism of gas discharge caused by triboelectrification and contact electrification is not clearly understood in the literature, and the generation of charged interfaces by contact–separation or friction has been attributed to the transfer of electrons, ions or charged fragments of polymer chains on the interfaces between two materials.[70–72]

Considering our previous report on common luminophore excitation in blended amorphous polymer films in which triboelectrification of the blended polymer matrix was proposed,[18] we then set out to compare the performance of the films

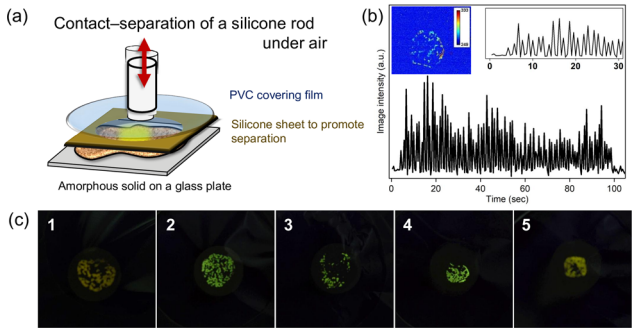

Fig. 8 (a) Schematic illustration of the experimental setup for luminescence generation by contact–separation of a silicone rod on a covering film placed on an amorphous solid; (b) luminescence imaging of ML of **3** (in pseudo color based on grayscale pixel intensity) and the time profile of the average image intensity of ML during repeated cycles of contact–separation monitored using a CCD camera; (c) photographs of the ML of **1–5** generated upon separation of the rod under air. The photographs were taken at 30 fps.

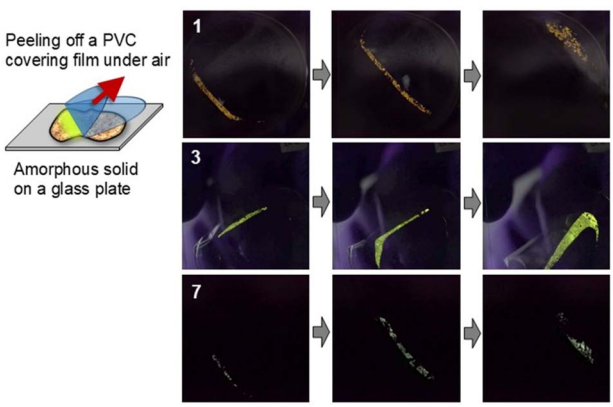

Fig. 9 Schematic illustration of the ML experiment and photographs of the ML generated by peeling off a PVC covering film (thickness: *ca.* 20 μm) placed on the surface of the amorphous solid films of **1**, **3**, and **7** on a glass plate under air. The photographs were taken at 30 fps.

composed of pure, amorphous Cu^{I} complexes, with polymer amorphous films physically blended with **1–8** (8 wt%). ML was observed by rubbing the surface of PMMA films containing **1–8** (8 wt%) under an inert atmosphere (Fig. S82–S84); however, contact–separation and peeling off a PVC covering film did not generate visible ML. In the case of **3**, enhancement of ML intensity was observed upon increasing the ratio of **3** in PMMA (10, 30, 50, 70, and 90 wt%) by friction. Overall, these results show that the presence of a polymer matrix is not essential for ML generation in amorphous solids.

The generality of ML in amorphous solids was further investigated using additional common metal complexes and organic luminophores (Fig. 10). XRD analysis of the obtained thin films on glass plates, which were prepared by spin coating, confirmed the presence of crystalline peaks for six of the eight samples (Fig. S62), thus showing that the preparation of purely amorphous samples is not always possible. Among them, cationic triphenylpyrylium tetrafluoroborate (**TPP**) and tris(1,10-phenanthroline)ruthenium(II) bis(hexafluorophosphate) (**[Ru(phen)$_3$](PF$_6$)$_2$**) did not show detectable ML by direct friction with a glass or a PFA tube under Ar (Fig. S87 and S88). However, all the additional eight reference PL compounds showed detectable ML by friction with a glass tube *via* a PVC covering film under air (Fig. S89 and S90), indicating the dependence of ML on a combination of materials used for triboelectrification. The generation of apparent visible ML by contact–separation was observed for **BBOT**, **DPVBi**, **Eu(dbm)$_3$(phen)**, **TPBD**, **TPP**, and **VB2TB** (Fig. S91). ML by peeling off a PVC covering film was also observed for the reference PL compounds except **[Ru(phen)$_3$](PF$_6$)$_2$** (Fig. S92 and S93), demonstrating that ML materials can be prepared by a simple method using non-crystalline solids of common PL compounds, and that ML from PL compounds can be generated without fracturing the crystalline solids.

ML in thin film-shaped solids of non-crystalline PL compounds generated by triboelectrification and contact electrification enables fabrication of flexible ML materials. To demonstrate the versatility of this approach, PL compounds were coated on a flexible PET film, which generated ML by friction, for example, *via* a polypropylene bag using a naked finger under air (Fig. 11 and SI Movie 7). Moreover, when a double-film system with PL compounds coated on a PET film covered with a PVC layer was used, ML generation was confirmed by bending and twisting (Fig. 12, S94, S95 and SI Movie 8). This was also seen when other common PL compounds were used. Control experiments without the PVC covering film showed no ML by bending, indicating that triboelectrification and contact electrification between the PL compound on the PET film and the outer PVC covering film are involved. When the outer covering film composed of PMMA, PS, PCL, or PBAC was placed, visible ML generation from the Cu^{I} complexes on the PET film by bending and twisting was not observed, suggesting that ML generation depends largely on the nature of two materials (*e.g.* position in triboelectric series) in contact rather than their flexibility or other properties, consistent with electrification induced by mechanical stimuli being the leading factor. The irregular pattern of instant ML generation upon bending and twisting the films is confirmed by SI Movie 8. We believe that further optimization of the materials will provide ML materials exhibiting more sensitive and brighter luminescence under various mechanical actions, using a wide range of common luminophores and polymers.

The previously reported molecular ML materials emit light by fracture of the crystalline solids, which imposes limitations on their technical implementation, not only because of the difficulty in the incorporation of well-defined crystals, but also due to the non-repeatable ML generation caused by destructive mechanical stimuli such as fracture and size-dependent intensity. The current finding demonstrates that ML can be generated from non-crystalline PL solids by non-destructive mechanical stimuli, such as contact–separation *via* an inert covering layer, bending, and twisting of the films, which may pave the way for practical applications of ML materials. As a demonstration of practical performance, we prepared a screen made of an amorphous film of complex **3** coated on glass, and sandwiched with a PVC cover, which was used to write letters instantly by applying pressure with a flexible silicon rod (or a bare finger), without any external source of energy (Fig. S96 and SI Movie 10). This experiment demonstrates the potential of

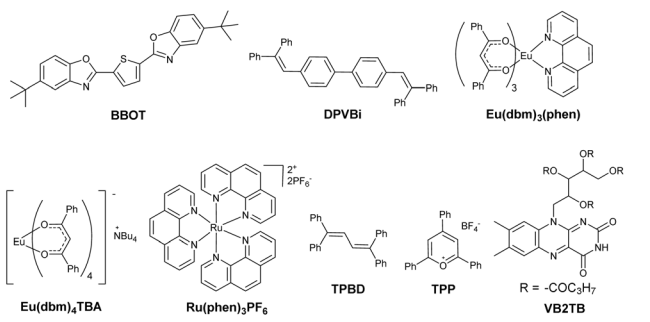

Fig. 10 Chemical structures of reference common PL compounds (alphabetical order).

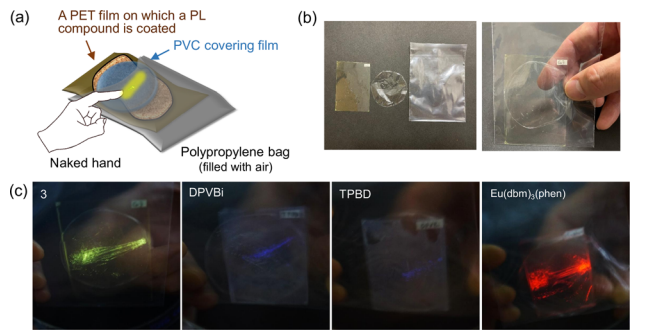

Fig. 11 (a) Schematic illustration of the ML experiment with flexible films; (b) photographs of the sample used for the experiment; (c) photographs of the ML of **3**, **DPVBi**, **TPBD** and **Eu(dbm)$_3$(phen)** coated on a polyethylene terephthalate (PET) film covered with a PVC film, which was generated by rubbing the surface of the outer polypropylene bag with a naked finger under air (27 °C, relative humidity: 31%). The exposure time of the camera for ML is 5 s.

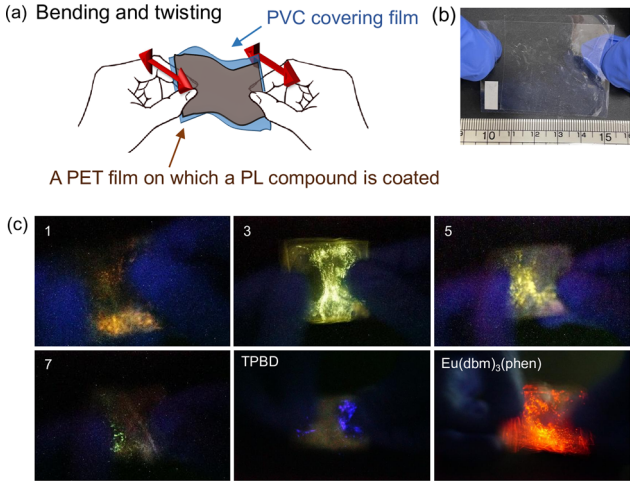

Fig. 12 (a) Schematic illustration of the ML experiment; (b) a photograph of a PET/PVC film sample used for the experiment; (c) photographs of the ML generated by bending and twisting under air. The exposure time of the camera for ML is 5 s.

ML for developing smart windows and displays that operate by mechanical actions without external electrical power, as well as mechanical sensors capable of visualizing subtle mechanical stimuli. This study also highlights that triboelectrification and contact electrification, along with other phenomena based on static electricity,[64] play an increasingly important role in studying and application of ML.

Conclusions

We demonstrated that heteroleptic Cu^{I} complexes **1–8** show ML as amorphous solids without being embedded in a polymer matrix, generated either by friction directly applied to the films, or through a PVC layer without direct physical friction damage; this ML generation is independent of ML properties in the crystalline phase, showing that the fracture of crystalline solids is not required in ML generation by this method. The presence of intense surrounding gas discharge luminescence peaks in the ML spectra of amorphous solids and the dependence of ML on the combination of materials used for friction implies that a localized electric field generated at the contact area by tribocharging, likely leads to Cu^{I} complex excitation. Contact–separation, or peeling off (separating) of a polymer film physically placed on the surface of the amorphous PL solids also generates ML, which is a new type of mechanoresponse reported for PL compounds. These ML properties can be further generalized by utilizing other common organic and coordination compounds. The current findings enable a convenient and simple approach to the generation of ML even under ambient conditions, which may find applications in the development of flexible mechanoresponsive materials that emit light under various mechanical stimuli, and in the visualization of electrical phenomena induced by mechanical actions, such as heterogeneous local charge distribution and discharge on material surfaces[61,69] caused by triboelectrification or contact electrification.

Author contributions

Ayumu Karimata: conceptualization, investigation, formal analysis, project administration, writing – review & editing. Daniil Ilatovskii: investigation, formal analysis (preparation of amorphous solids). Robert R. Fayzullin: investigation, formal analysis (X-ray analysis). Shinya Komoto: investigation, formal analysis (Images of ML, microscope images). Andrew Bruhacs: investigation, formal analysis (PL lifetime). Eugene Khaskin: investigation, formal analysis (X-ray analysis). Julia R. Khusnutdinova: supervision, resources, funding acquisition, project administration, writing – review & editing.

Conflicts of interest

There are no conflicts to declare.

Data availability

CCDC 2449099–2449107 (**1–8B**) contain the supplementary crystallographic data for this paper.[73]

The data supporting this study have been included as part of the supplementary information (SI), including supplementary movies. Supplementary information is available. See DOI: **https://doi.org/10.1039/d5sc05673j**.

Acknowledgements

We thank Dr Hyung Been Kang (MEMS, OIST), the Mechanical Engineering Section and the Instrumental Analysis Section at OIST for technical support, and OIST for funding. R. R. F. performed crystal structure determination under the assignment to the FRC Kazan Scientific Center of RAS.

Notes and references

1 J. I. Zink, Triboluminescence, *Acc. Chem. Res.*, 1978, **11**, 289–295.
2 I. Sage and G. Bourhill, Triboluminescent materials for structural damage monitoring, *J. Mater. Chem.*, 2001, **11**, 231–245.
3 D. O. Olawale, J. Uddin, J. Yan, T. Dickens and O. Okoli, *Triboluminescence*, Springer, 2016.
4 Y. Xie and Z. Li, Triboluminescence: Recalling Interest and New Aspects, *Chem*, 2018, **4**, 943–971.
5 J.-C. G. Bunzli and K.-L. Wong, Lanthanide mechanoluminescence, *J. Rare Earths*, 2018, **36**, 1–41.
6 S. Mukherjee and P. Thilagar, Renaissance of Organic Triboluminescent Materials, *Angew. Chem., Int. Ed.*, 2019, **58**, 7922–7932.
7 Y. Zhuang and R. J. Xie, Mechanoluminescence Rebrightening the Prospects of Stress Sensing: A Review, *Adv. Mater.*, 2021, **33**, e2005925.
8 L. Su, H. J. Wang and Y. L. Zi, Recent progress of triboelectrification-induced electroluminescence: from fundaments to applications, *J. Phys Mater.*, 2021, **4**, 042001.

9 Y. Hirai, On Sense and Deform: Molecular Luminescence for Mechanoscience, *ACS Appl. Opt. Mater.*, 2024, **2**, 1025–1045.
10 W. Wang, J. Tan, H. Wang, H. Xiao, R. Shen, B. Huang and Q. Yuan, Self-Powered and Self-Recoverable Multimodal Force Sensors Based on Trap State and Interfacial Electron Transfer, *Angew. Chem., Int. Ed.*, 2024, **63**, e202404060.
11 N. Takada, J. Sugiyama, R. Katoh, N. Minami and S. Hieda, Mechanoluminescent properties of europium complexes, *Synth. Met.*, 1997, **91**, 351–354.
12 R. S. Fontenot, W. A. Hollerman, K. N. Bhat, M. D. Aggarwal and B. G. Penn, Incorporating strongly triboluminescent europium dibenzoylmethide triethylammonium into simple polymers, *Polym. J.*, 2014, **46**, 111–116.
13 T. M. George, M. J. Sajan, N. Gopakumar and M. L. P. Reddy, Bright red luminescence and triboluminescence from PMMA-doped polymer film materials supported by Eu -triphenylphosphine based β-diketonate and 4,5-bis(diphenylphosphino)-9,9-dimethylxanthene oxide, *J. Photochem. Photobiol., A*, 2016, **317**, 88–99.
14 A. İncel, M. Emirdag-Eanes, C. D. McMillen and M. M. Demir, Integration of Triboluminescent EuD4TEA Crystals to Transparent Polymers: Impact Sensor Application, *ACS Appl. Mater. Interfaces*, 2017, **9**, 6488–6496.
15 A. İncel, C. Varlikli, C. D. McMillen and M. M. Demir, Triboluminescent Electrospun Mats with Blue-Green Emission under Mechanical Force, *J. Phys. Chem. C*, 2017, **121**, 11709–11716.
16 X. Liu, C. Ge, Z. Yang, Y. Song, A. Wang, Y. Kang, B. Li and Q. Dong, Guanidine-Templated Manganese Halides Single Crystals toward Efficient Mechanoluminescence and Photoluminescence by Supramolecular Interactions Modulation, *Adv. Opt. Mater.*, 2021, **9**, 2100862.
17 A. Karimata, P. H. Patil, R. R. Fayzullin, E. Khaskin, S. Lapointe and J. R. Khusnutdinova, Triboluminescence of a new family of Cu(I)-NHC complexes in crystalline solid and in amorphous polymer films, *Chem. Sci.*, 2020, **11**, 10814–10820.
18 A. Karimata, R. R. Fayzullin and J. R. Khusnutdinova, Versatile Method of Generating Triboluminescence in Polymer Films Blended with Common Luminophores, *ACS Macro Lett.*, 2022, **11**, 1028–1033.
19 F. A. Cotton, M. Goodgame and D. M. Goodgame, Absorption Spectra and Electronic Structures of Some Tetrahedral Manganese(II) Complexes, *J. Am. Chem. Soc.*, 1962, **84**, 167–172.
20 F. A. Cotton, L. M. Daniels and P. Huang, Correlation of Structure and Triboluminescence for Tetrahedral Manganese(II) Compounds, *Inorg. Chem.*, 2001, **40**, 3576–3578.
21 C.-W. Hsu, K. T. Ly, W.-K. Lee, C.-C. Wu, L.-C. Wu, J.-J. Lee, T.-C. Lin, S.-H. Liu, P.-T. Chou, G.-H. Lee and Y. Chi, Triboluminescence and Metal Phosphor for Organic Light-Emitting Diodes: Functional Pt(II) Complexes with Both 2-Pyridylimidazol-2-ylidene and Bipyrazolate Chelates, *ACS Appl. Mater. Interfaces*, 2016, **8**, 33888–33898.
22 K. Sasaki, D. Saito, M. Yoshida, F. Tanaka, A. Kobayashi, K. Sada and M. Kato, Chromic triboluminescence of self-assembled platinum(ii) complexes, *Chem. Commun.*, 2023, **59**, 6745–6748.
23 G. L. Sharipov and A. A. Tukhbatullin, Triboluminescence of tris(2,2′-bipyridyl)ruthenium(II) dichloride hexahydrate, *J. Lumin.*, 2019, **215**, 116691.
24 D. M. Knotter, H. L. Van Maanen, D. M. Grove, A. L. Spek and G. Van Koten, Synthesis and properties of trimeric ortho-chelated (arenethiolato)copper(I) complexes, *Inorg. Chem.*, 1991, **30**, 3309–3317.
25 F. Marchetti, C. Di Nicola, R. Pettinari, I. Timokhin and C. Pettinari, Synthesis of a Photoluminescent and Triboluminescent Copper(I) Compound: An Experiment for an Advanced Inorganic Chemistry Laboratory, *J. Chem. Educ.*, 2012, **89**, 652–655.
26 M. Hoshino and Y. Ohgo, Investigating the Mechanism of Triboluminescence: Insights from Structural and Electrostatic Characterization of Copper Thiocyanate Complexes, *Chem.–Eur. J.*, 2024, **30**, e202401715.
27 L. Tu, Y. Xie and Z. Li, Advances in Pure Organic Mechanoluminescence Materials, *J. Phys. Chem. Lett.*, 2022, **13**, 5605–5617.
28 R. Czerwieniec, M. J. Leitl, H. H. H. Homeier and H. Yersin, Cu(I) complexes – thermally activated delayed fluorescence. Photophysical approach and material design, *Coord. Chem. Rev.*, 2016, **325**, 2–28.
29 Y. Zhang, M. Schulz, M. Wächtler, M. Karnahl and B. Dietzek, Heteroleptic diimine–diphosphine Cu(I) complexes as an alternative towards noble-metal based photosensitizers: design strategies, photophysical properties and perspective applications, *Coord. Chem. Rev.*, 2018, **356**, 127–146.
30 J. Beaudelot, S. Oger, S. Peruško, T.-A. Phan, T. Teunens, C. Moucheron and G. Evano, Photoactive Copper Complexes: Properties and Applications, *Chem. Rev.*, 2022, **122**, 16365–16609.
31 S.-M. Kuang, D. G. Cuttell, D. R. McMillin, P. E. Fanwick and R. A. Walton, Synthesis and Structural Characterization of Cu(I) and Ni(II) Complexes that Contain the Bis[2-(diphenylphosphino)phenyl]ether Ligand. Novel Emission Properties for the Cu(I) Species, *Inorg. Chem.*, 2002, **41**, 3313–3322.
32 K. Kubiček, S. T. Veedu, D. Storozhuk, R. Kia and S. Techert, Geometric and electronic properties in a series of phosphorescent heteroleptic Cu(I) complexes: crystallographic and computational studies, *Polyhedron*, 2017, **124**, 166–176.
33 T.-H. Huang, C. Luo and D. Zheng, Luminescent cationic/neutral Cu(I) complexes for use in light-emitting diodes: synthesis, structural characterization, DFT studies and properties, *Org. Electron.*, 2021, **97**, 106273.
34 L. Donato, Y. Atoini, E. A. Prasetyanto, P. Chen, C. Rosticher, C. Bizzarri, K. Rissanen and L. De Cola, Selective Encapsulation and Enhancement of the Emission Properties of a Luminescent Cu(I) Complex in Mesoporous Silica, *Helv. Chim. Acta*, 2018, **101**, e1700273.
35 C. W. Hsu, C. C. Lin, M. W. Chung, Y. Chi, G. H. Lee, P. T. Chou, C. H. Chang and P. Y. Chen, Systematic

investigation of the metal-structure-photophysics relationship of emissive d10-complexes of group 11 elements: the prospect of application in organic light emitting devices, *J. Am. Chem. Soc.*, 2011, **133**, 12085–12099.
36 Deposition numbers CCDC 2449099 (**1**), 2449100 (**2**), 2449101 (**3**), 2449102 (**4**), 2449103 (**5**), 2449104 (**6**), 2449105 (**7**), 2449106 (**8A**), and 2449107 (**8B**) contain the supplementary crystallographic data for this paper.
37 M.-H. Wang, T. Konya, M. Yahata, Y. Sawada, A. Kishi, T. Uchida, H. Lei, Y. Hoshi and L.-X. Sun, Thermal change of organic light-emitting ALQ3 thin films, *J. Therm. Anal. Calorim.*, 2010, **99**, 117–122.
38 M. Shibata, Y. Sakai and D. Yokoyama, Advantages and disadvantages of vacuum-deposited and spin-coated amorphous organic semiconductor films for organic light-emitting diodes, *J. Mater. Chem. C*, 2015, **3**, 11178–11191.
39 M. G. Crestani, G. F. Manbeck, W. W. Brennessel, T. M. McCormick and R. Eisenberg, Synthesis and Characterization of Neutral Luminescent Diphosphine Pyrrole- and Indole-Aldimine Copper(I) Complexes, *Inorg. Chem.*, 2011, **50**, 7172–7188.
40 J. Li, L. Wang, Z. Zhao, X. Li, X. Yu, P. Huo, Q. Jin, Z. Liu, Z. Bian and C. Huang, Two-Coordinate Copper(I)/NHC Complexes: Dual Emission Properties and Ultralong Room-Temperature Phosphorescence, *Angew. Chem., Int. Ed.*, 2020, **59**, 8210–8217.
41 M. Ghosh, J. Chatterjee, P. Panwaria, A. Kudlu, S. Tothadi and S. Khan, Silylene-Copper-Amide Emitters: From Thermally Activated Delayed Fluorescence to Dual Emission, *Angew. Chem., Int. Ed.*, 2024, **63**, e202410792.
42 X.-M. Zeng, M. Wu, L.-Y. Yao and G.-Y. Yang, Dynamic Phosphorescence Behavior of Carbene-Metal-Amide Complexes from the Perspective of Excited State Modulation, *Angew. Chem., Int. Ed.*, 2025, **64**, e202419614.
43 J.-i. Nishida, H. Ohura, Y. Kita, H. Hasegawa, T. Kawase, N. Takada, H. Sato, Y. Sei and Y. Yamashita, Phthalimide Compounds Containing a Trifluoromethylphenyl Group and Electron-Donating Aryl Groups: Color-Tuning and Enhancement of Triboluminescence, *J. Org. Chem.*, 2016, **81**, 433–441.
44 F. G. Wick, Triboluminescence of Sugar, *J. Opt. Soc. Am.*, 1940, **30**, 302–306.
45 L. M. Belyaev and Y. N. Martyshev, Triboluminescence of Some Alkali Halide Crystals, *Phys. Status Solidi B*, 1969, **34**, 57–62.
46 E. N. Harvey, The Luminescence of Adhesive Tape, *Science*, 1939, **89**, 460–461.
47 B. P. Chandra and J. I. Zink, Triboluminescence of inorganic sulfates, *Inorg. Chem.*, 1980, **19**, 3098–3102.
48 A. A. Tukhbatullin, G. L. Sharipov, A. M. Abdrakhmanov and M. R. Muftakhutdinov, Mechanoluminescence of terbium and cerium sulfates in a noble-gas atmosphere, *Opt. Spectrosc.*, 2014, **116**, 691–694.
49 A. A. Tukhbatullin, G. L. Sharipov and R. A. Nevshupa, Non-trivial role of surrounding gases in triboluminescence: a comprehensive review, *Friction*, 2025, **13**, 9440998.
50 L. M. Sweeting, Triboluminescence with and without air, *Chem. Mater.*, 2001, **13**, 854–870.
51 K. Nakayama and R. A. Nevshupa, Characteristics and Pattern of Plasma Generated at Sliding Contact, *J. Tribol.*, 2003, **125**, 780–787.
52 K. Nakayama and R. A. Nevshupa, Effect of dry air pressure on characteristics and patterns of tribomicroplasma, *Vacuum*, 2004, **74**, 11–17.
53 D. Puhan, R. Nevshupa, J. S. S. Wong and T. Reddyhoff, Transient aspects of plasma luminescence induced by triboelectrification of polymers, *Tribol. Int.*, 2019, **130**, 366–377.
54 K. i. Hiratsuka and K. Hosotani, Effects of friction type and humidity on triboelectrification and triboluminescence among eight kinds of polymers, *Tribol. Int.*, 2012, **55**, 87–99.
55 H. Suzuki, D. C. Zou, T. Izumi, H. Yamamoto, X. T. Tao, T. Watanabe, H. Usui and S. Miyata, Luminescence of dye-doped polymer films induced by corona discharge, *J. Appl. Phys.*, 2000, **88**, 5791–5795.
56 A. F. Diaz and R. M. Felix-Navarro, A semi-quantitative tribo-electric series for polymeric materials: the influence of chemical structure and properties, *J. Electrost.*, 2004, **62**, 277–290.
57 H. Zou, Y. Zhang, L. Guo, P. Wang, X. He, G. Dai, H. Zheng, C. Chen, A. C. Wang, C. Xu and Z. L. Wang, Quantifying the triboelectric series, *Nat. Commun.*, 2019, **10**, 1427.
58 B. A. Kwetkus, K. Sattler and H. C. Siegmann, Gas breakdown in contact electrification, *J. Phys. D: Appl. Phys.*, 1992, **25**, 139.
59 R. G. Horn and D. T. Smith, Contact Electrification and Adhesion Between Dissimilar Materials, *Science*, 1992, **256**, 362–364.
60 L. S. McCarty and G. M. Whitesides, Electrostatic Charging Due to Separation of Ions at Interfaces: Contact Electrification of Ionic Electrets, *Angew. Chem., Int. Ed.*, 2008, **47**, 2188–2207.
61 Y. I. Sobolev, W. Adamkiewicz, M. Siek and B. A. Grzybowski, Charge mosaics on contact-electrified dielectrics result from polarity-inverting discharges, *Nat. Phys.*, 2022, **18**, 1347–1355.
62 H.-J. Park, S. Kim, J. H. Lee, H. T. Kim, W. Seung, Y. Son, T. Y. Kim, U. Khan, N.-M. Park and S.-W. Kim, Self-Powered Motion-Driven Triboelectric Electroluminescence Textile System, *ACS Appl. Mater. Interfaces*, 2019, **11**, 5200–5207.
63 N. Wang, M. Pu, Z. Ma, Y. Feng, Y. Guo, W. Guo, Y. Zheng, L. Zhang, Z. Wang, M. Feng, X. Li and D. Wang, Control of triboelectricity by mechanoluminescence in ZnS/Mn-containing polymer films, *Nano Energy*, 2021, **90**, 106646.
64 K. Kikunaga and N. Terasaki, Demonstration of static electricity induced luminescence, *Sci. Rep.*, 2022, **12**, 8524.
65 C. Li, N. Schramma, Z. Wang, N. F. Qari, M. Jalaal, M. I. Latz and S. Cai, Ultrasensitive and robust mechanoluminescent living composites, *Sci. Adv.*, 2023, **9**, eadi8643.
66 C. Li, Q. He, Y. Wang, Z. Wang, Z. Wang, R. Annapooranan, M. I. Latz and S. Cai, Highly robust and soft biohybrid

mechanoluminescence for optical signaling and illumination, *Nat. Commun.*, 2022, **13**, 3914.

67 A. J. Alexander, Interfacial Ion-Transfer Mechanism for the Intense Luminescence Observed When Opening Self-Seal Envelopes, *Langmuir*, 2012, **28**, 13294–13299.

68 K. Brörmann, B. Karin, J. Anand and R. Bennewitz, Discharge During Detachment of Micro-Structured PDMS Sheds Light on the Role of Electrostatics in Adhesion, *J. Adhes.*, 2012, **88**, 589–607.

69 M. P. Reiter and T. Shinbrot, Paradoxical peeling patterns, *Sci. Rep.*, 2024, **14**, 20524.

70 F. Galembeck, T. A. L. Burgo, L. B. S. Balestrin, R. F. Gouveia, C. A. Silva and A. Galembeck, Friction, tribochemistry and triboelectricity: recent progress and perspectives, *RSC Adv.*, 2014, **4**, 64280–64298.

71 D. J. Lacks and T. Shinbrot, Long-standing and unresolved issues in triboelectric charging, *Nat. Rev. Chem.*, 2019, **3**, 465–476.

72 J. Zhang, C. Su, F. J. M. Rogers, N. Darwish, M. L. Coote and S. Ciampi, Irreproducibility in the triboelectric charging of insulators: evidence of a non-monotonic charge versus contact time relationship, *Phys. Chem. Chem. Phys.*, 2020, **22**, 11671–11677.

73 CCDC 2449099: Experimental Crystal Structure Determination, 2025, DOI: **10.5517/ccdc.csd.cc2n6h6l**; CCDC 2449100: Experimental Crystal Structure Determination, 2025, DOI: **10.5517/ccdc.csd.cc2n6h7m**; CCDC 2449101: Experimental Crystal Structure Determination, 2025, DOI: **10.5517/ccdc.csd.cc2n6h8n**; CCDC 2449102: Experimental Crystal Structure Determination, 2025, DOI: **10.5517/ccdc.csd.cc2n6h9p**; CCDC 2449103: Experimental Crystal Structure Determination, 2025, DOI: **10.5517/ccdc.csd.cc2n6hbq**; CCDC 2449104: Experimental Crystal Structure Determination, 2025, DOI: **10.5517/ccdc.csd.cc2n6hcr**; CCDC 2449105: Experimental Crystal Structure Determination, 2025, DOI: **10.5517/ccdc.csd.cc2n6hds**; CCDC 2449106: Experimental Crystal Structure Determination, 2025, DOI: **10.5517/ccdc.csd.cc2n6hft**; CCDC 2449107: Experimental Crystal Structure Determination, 2025, DOI: **10.5517/ccdc.csd.cc2n6hgv**.